Available online at www.sciencedirect.com
ScienceDirect
Life Sciences 81 (2007) 1332–1338
Life Sciences
www.elsevier.com/locate/lifescie

# Emodin-mediated protection from acute myocardial infarction via inhibition of inflammation and apoptosis in local ischemic myocardium

Yanxia Wu [a,1], Xin Tu [b,1], Guosheng Lin [a], Hao Xia [a], Hao Huang [c], Jing Wan [d], Zhide Cheng [e], Mengyuan Liu [e], Gao Chen [e], Haimou Zhang [e], Jinrong Fu [a], Qian Liu [d], Dong-xu Liu [e,*]

[a] Department of Cardiology, Renmin Hospital of Wuhan University, Wuhan, Hubei, PR China
[b] Human Genome Research Center, Huazhong University of Science and Technology, Wuhan, Hubei, PR China
[c] The First Hospital of Wuhan, Wuhan, Hubei, PR China
[d] Department of Cardiology, Zhongnan Hospital of Wuhan University, Wuhan, Hubei, PR China
[e] Center for Infection and Immunity Research, School of Life Sciences, Hubei University, Wuhan, Hubei, PR China

Received 14 December 2006; accepted 20 August 2007

**Abstract**

Acute myocardial infarction (AMI) is associated with inflammation and apoptosis. Emodin plays an anti-inflammatory role in several inflammatory diseases. Recent studies have demonstrated that emodin protects against myocardial ischemia/reperfusion injury. However, its mechanism underlying its effects remains unknown. In a murine model of AMI, based on ligation of the left coronary artery, administration of emodin reduced myocardial infarct size (MIS) in a dose-dependent manner. Emodin significantly suppressed TNF-α expression and NF-κB activation in the local myocardial infarction area. Treatment with emodin inhibited myocardial cell apoptosis by inhibiting caspase-3 activation. Therefore, these studies demonstrate that emodin protects against myocardial cell injury via suppression of local inflammation and apoptosis.


*Keywords:* Emodin; Inflammation; Apoptosis; Myocardial infarction

## Introduction

Acute myocardial infarction (AMI) causes local inflammation and apoptosis (Frangogiannis et al., 2002), which results in myocardial cell damage (Nian et al., 2004). Proinflammatory mediators are up-regulated in cardiac dysfunction (Torre-Amione, 2005), and in particular, elevated TNF-α levels in the local infarct myocardium contribute to acute myocardial dysfunction and cause myocardial cell apoptosis (Sun et al., 2004; Krown et al., 1996). Apoptosis may persist in infarcted areas (Baldi et al., 2002; Palojoki et al., 2001). Therefore, inhibition of inflammation and apoptosis may be a therapeutic strategy for AMI.

Emodin (3-methyl-1, 6, 8-trihydroxyanthraquinone) is an active anthraquinone constituent of rhubarb extract and functions through anti-mutagenic, anti-cancer, anti-diuretic, vasorelaxant, and immunosuppressive activities (Chan et al., 1993; Koyama et al., 1988; Su et al., 1995; Zhou and Chen, 1988; Chen et al., 2004; Li et al., 2005). Recently, protection by emodin from both cerebral ischemia injury and myocardial ischemia/reperfusion injury was associated with the inhibition of inflammation (Lu et al., 2005; Du and Ko, 2005). In this study, we demonstrate that emodin inhibits inflammation and apoptosis in local myocardial cell injury.

## Materials and methods

### *Model of AMI in mice*

Male BALB/c mice (18–25 g, 8–12 weeks) were purchased from the Experimental Animal Center of Hubei Province, Wuhan, China. Mice were housed in a facility with a 12/12 h light/dark cycle. The room was kept specific pathogen free. All animals were handled in accordance with the Guide for the Local Care and Use of Laboratory Animals. AMI was produced

* Corresponding author. Center for Infection and Immunity Research, School of Life Sciences, Hubei University, 11 XueYuan Road, Wuhan, Hubei, PR China. Tel.: +86 27 88663882; fax: 86 27 88663110.
*E-mail address:* dxliu@hubu.edu.cn (D. Liu).
[1] Yanxia Wu and Xin Tu contributed equally to this work.

0024-3205/$ - see front matter © 2007 Published by Elsevier Inc.
doi:10.1016/j.lfs.2007.08.040

by occluding the left anterior descending coronary artery according to a previously described method (Tarnavski et al., 2004) with minor modifications. Briefly, mice were anesthetized with 0.2–0.4 ml of pentobarbital sodium solution (4 mg/ml) given intraperitoneally. Animals were intubated with a 24GA intravenous catheter and ventilated with a rodent ventilator (DW-2000 Apparatus, Shanghai). Each animal was placed in a supine position with paws taped to an electrocardiogram (ECG) board (lead I, aVL) to measure S–T segment elevations during AMI. AMI was produced by permanent ligation of the left coronary artery (LCA) with an 8-0 nylon surgical suture. Successful ligation of the LCA was verified visually by color change in the ischemic area and ECG lead I and aVL S–T segment elevations after the occlusion. Sham-operated mice were prepared in the same manner, but no coronary ligation was performed. After recovering from anesthesia, the animals were maintained in an air-conditioned room.

*Drug administration*

Emodin (provided by Professor Zhang Xiping, from the Department of General Surgery in Hangzhou No. 1 Hospital) was dissolved in dimethylsulfoxide (DMSO) (Sigma Chemical, USA), further diluted to a final concentration of 200 mg/ml, and injected intraperitoneally 1 h before left anterior descending coronary artery occlusion. For long-term survival studies (2 weeks), the animals received a second injection of emodin 24 h after AMI. The animals that received administration of emodin or DMSO (vehicle) were assigned randomly to experimental groups comprising six mice each. To determine the optimal efficacy dose of emodin in the AMI model, different doses were administered as described above, beginning at 1 h before the onset of occlusion, and all animals received a second dose at 24 h after ischemia. Emodin concentrations were 3.75, 7.5, 15, 30, and 60 mg/kg.

*Morphological examination*

Infarct size was evaluated with the triphenyltetrazolium chloride (TTC)–Evans blue technique (Shiomi et al., 2004). At the end of each experiment, the artery was reoccluded with the exception of the sham group. Evans blue (1.5 ml of a 1.0% solution) was injected intravenously to separate the left ventricular (LV) area at risk (AAR) for infarction from surrounding normal areas. Hearts were excised and sliced into cross sections from the base to apical tip with the first cutter blade positioned at the site of coronary artery occlusion. The heart sections were incubated with 1% triphenyltetrazolium chloride solution (Sigma-Aldrich, USA) at 37 °C for 15 min. The infarct area (IA), AAR, and total LV area were measured in each section using Image-pro plus 5.0. Ratios of IA/LV and IA/AAR were calculated and expressed as percentages. Myocardial infarct size was expressed as a percentage of LV mass and of the AAR. Two weeks after surgery, the hearts were excised and fixed with 4% paraformaldehyde (Sigma-Aldrich, USA). Hearts were cut serially from apex to base. To assess polymorphonuclear neutrophil (PMN) infiltration, sections stained with hematoxylin and eosin were observed microscopically, and the number of PMNs were counted in 3 to 5 fields for each heart (Hoffmeyer et al., 2000). For each of the hearts examined, the number of PMNs was counted in the infarcted zone (LV anterior wall) in six fields of three independent tissue sections by a blinded observer. Quantitation of myocardial cell apoptosis was achieved using a commercially available in situ cell death detection kit (Roche Applied Science, Indianapolis, IN) to find DNA strand breaks using the terminal deoxynucleotidyl transferase-mediated dUTP nick end labeling (TUNEL) reagent according to the manufacturer's protocol. Positive apoptotic nuclei were stained brown in infarcted myocardial tissue.

*Myocardium myeloperoxidase (MPO) activity assay*

The concentration of MPO was determined according to the MPO detection kit instructions (Nanjing Bioengineering Institute, Jiancheng, China) and was used as an index of neutrophil accumulation in the myocardium.

*Quantitative reverse transcription-polymerase chain reaction (QRT-PCR)*

TNF-α mRNA levels were determined by QRT-PCR using a QuantiTect SYBR Green RT-PCR Kit (Qiagen Ltd) on a LightCycler (Roche Diagnostics Ltd., Lewes, UK). Total RNA was isolated from samples (LV) with Trizol reagent (Gibco BRL) according to the manufacturer's instructions. Primers were designed to generate short amplification products (251 bp

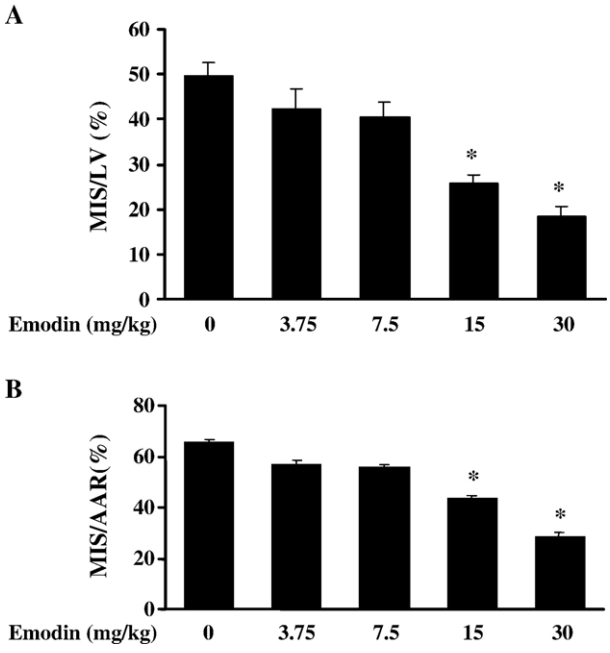


Fig. 1. Emodin reduces MIS in mice. Mice undergoing AMI were injected with emodin at concentrations of 0, 3.75, 7.5, 15, and 30 mg/kg. Myocardial infarct size (MIS) was measured based on the regional loss of TTC–Evans blue staining in heart sections at 2 weeks after AMI. (A) AAR/LV, ratio of area at risk (AAR) to total left ventricular (LV) area; (B) MIS/AAR, ratio of myocardial infarct size (MIS) to AAR. Data are expressed as a mean±s.e.m. ($n$=6). All results presented are from independent experiments.

for TNF-α and 177 bp for GADPH, used as an internal standard), which spanned one intron to detect contamination by genomic DNA. The sequences of the specific primers were: TNF-α 5′-GGCCCAGACCCTCACACTCA-3′ and 5′-CATCGGCTGGCACCACTAGTT-3′; GADPH: 5′-AACTGAGGGCTCTGCTCGCT-3′ and 5′-GTGACACACCGCAAGGCTT-3′. RT-PCR was performed in 20 μl reactions using 10 pmol of primers. Reverse transcription was carried out at 50 °C for 20 min, and cDNA was amplified for 37 cycles: 94 °C for 10 s, 57 °C for 15 s, and 72 °C for 5 s. The relative quantity of gene expression was calculated according to the manufacturer's recommendations. GAPDH was used as an internal control to calculate the relative abundance of TNFα mRNA.

*Annexin V immunostaining and flow cytometric analysis*

To quantify apoptotic cardiac cells, FACS was applied using a single cell suspension prepared from LV tissue. Hearts were rapidly removed and immediately mounted on a temperature controlled (37 °C) Landendorff perfusion system, and ventricular myocytes were enzymatically dissociated as previously described (Zhou et al., 2000). The resulting cell suspension was filtered through a 200-μm metal mesh to remove tissue debris

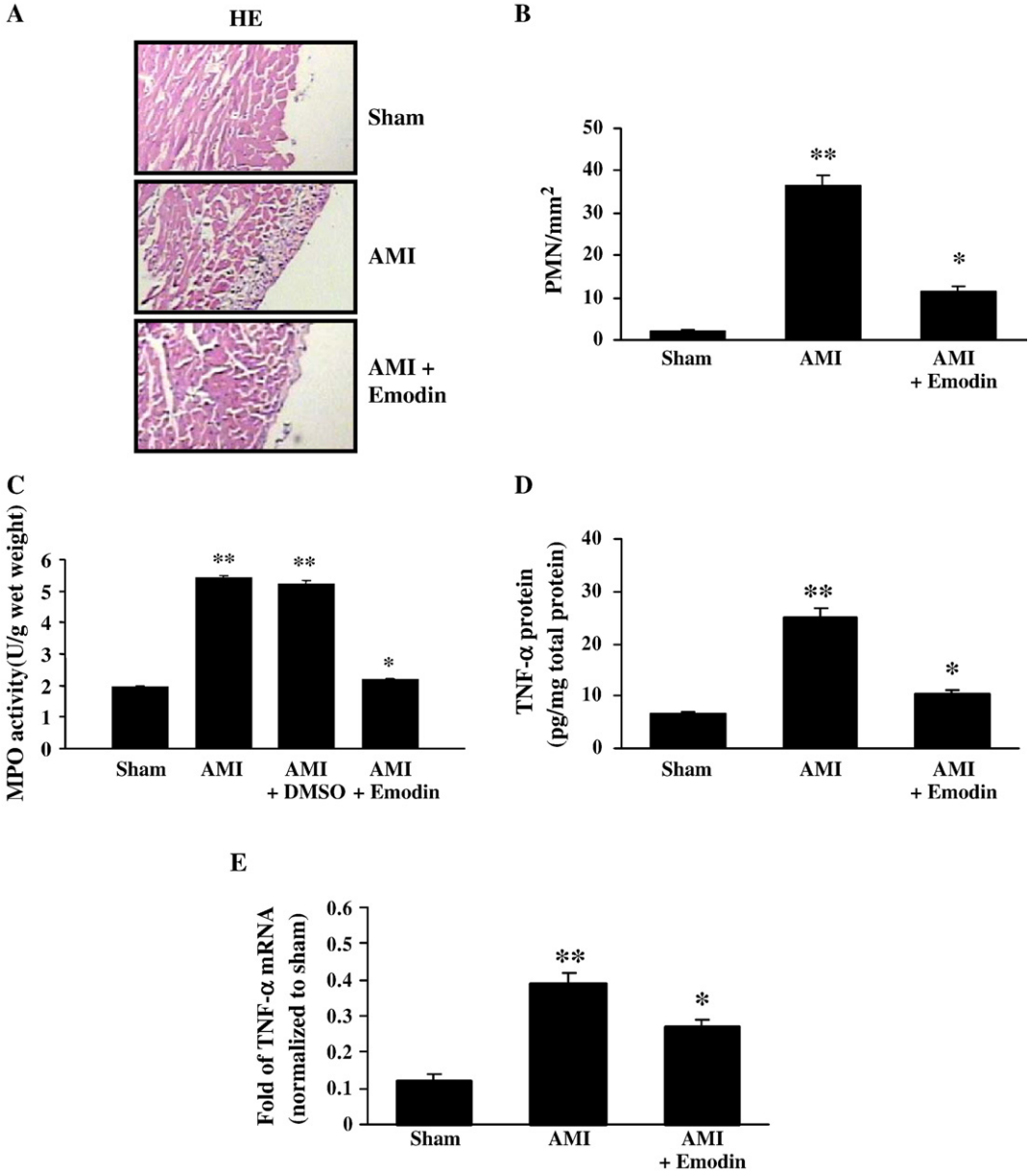


Fig. 2. Emodin inhibits the number of infiltrating PMNs and TNF-α expression. (A) Color photomicrographs of heart sections showing neutrophil infiltration in infarcted myocardial tissues (100×) 2 weeks after AMI. (B) The number of polymorphonuclear neutrophils was counted in sections stained with hematoxylin and eosin. (C) Infiltration of myocardial PMNs and a marker of MPO activity. (D) Levels of membrane-bound TNF-α protein were significantly decreased by ELISA. (E) Cytoplasmic TNF-α mRNA expression was analyzed by QRT-PCR. Data are expressed as a mean±s.e.m. ($n$=6). All results presented are from independent experiments.

and centrifuged at 1500 g for 1 min to remove the supernatant. This procedure routinely yielded >80% intact ventricular myocytes. At least 10,000 cardiac myocytes were examined. The concentration of cardiac myocytes was adjusted to $1 \times 10^6$/ml by addition of PBS. These cells were incubated with PE-conjugated Annexin V-FITC (5 μl, Bender) and 10 μl PI (20 μg/ml, Sigma Chemical) at 37 °C for 10 min. Fluorescence was measured on a FACScan flow cytometer (Becton Dickinson, USA) and analyzed with CellQuest software (Becton Dickinson, USA). All samples were measured and analyzed three times.

*Enzyme-linked immunosorbent assay (ELISA)*

Viable ventricular tissue was flash frozen in liquid nitrogen. Frozen tissue (50 mg) was homogenized, and membrane-bound TNF-α protein was collected (Torre-Amione et al., 1999). Myocardial TNF-α in the cardiac tissue was determined by ELISA with a commercially available ELISA kit (BD Biosciences, USA) according to the manufacturer's instructions. All samples and standards were measured in duplicate.

*Western blot*

Western blot analysis was performed to measure precaspase-3, active caspase-3, and P50 NF-κB proteins. Nuclear protein was extracted from LV myocardium tissue with a Nuclear Extraction Kit (Catalog No. 2900, CHEMICON, USA) according to the manufacturer's instructions. The membrane was incubated with caspase-3 (H-277) and NF-κB anti-p50 antibodies (Santa Cruz, USA), followed by incubation with horseradish peroxidase-conjugated anti-rabbit-IgG secondary antibody. Finally, the membrane was developed with the ECL-plus chemiluminescence detection system (Pierce, USA) by exposing it to roentgen-film in a dark room to visualize the bands. GAPDH was used as an internal control. The concentration of protein was obtained from the densitometry value of the corresponding band measured by TotalLab software (Nonlinear Dynamics, USA).

*Electrophoretic mobility shift assay (EMSA)*

EMSA was performed using a commercial kit (Gel Shift Assay System; Promega, Madison, WI). An NF-κB oligonucleotide probe (5′-AGTTGA GGG GAC TTT CCC AGG C-3′) was end-labeled with T4-polynucleotide kinase. Nuclear protein (10 μg) was preincubated in a total volume of 9 μl in binding buffer, consisting of 10 mM Tris–HCl (pH 7.5), 4% glycerol, 1 mM $MgCl_2$, 0.5 mM EDTA, 0.5 mM DTT, 0.5 mM NaCl, and 0.05 mg/ml poly (di–dc) for 15 min at room temperature. After adding the $^{32}$P-labeled oligonucleotide probe, the incubation was continued for an additional 20 min at room temperature. The reaction was stopped by adding 1 μl of gel loading buffer, and the mixture was subjected to nondenaturing 4% polyacrylamide gel electrophoresis in 0.5× TBE buffer. For supershift assays, nuclear proteins were incubated with anti-p50 antibody (1:500, Santa Cruz, USA) before the binding reaction. After electrophoresis was conducted at 380 V for 1 h, the gel was dried and exposed at −80 °C. These results were analyzed using NIH Image software.

*Statistical analysis*

All data are expressed as mean±s.e.m. All other comparisons were made using one-way ANOVA or *t*-test where appropriate. $P<0.05$ was considered a significant difference.

## Results

*Emodin reduces myocardial infarct size in mice*

A model of AMI was established in mice by ligating the left coronary artery. Myocardial infarct size (MIS) was expressed as a percentage of LV mass and of the AAR at 2 weeks after AMI.

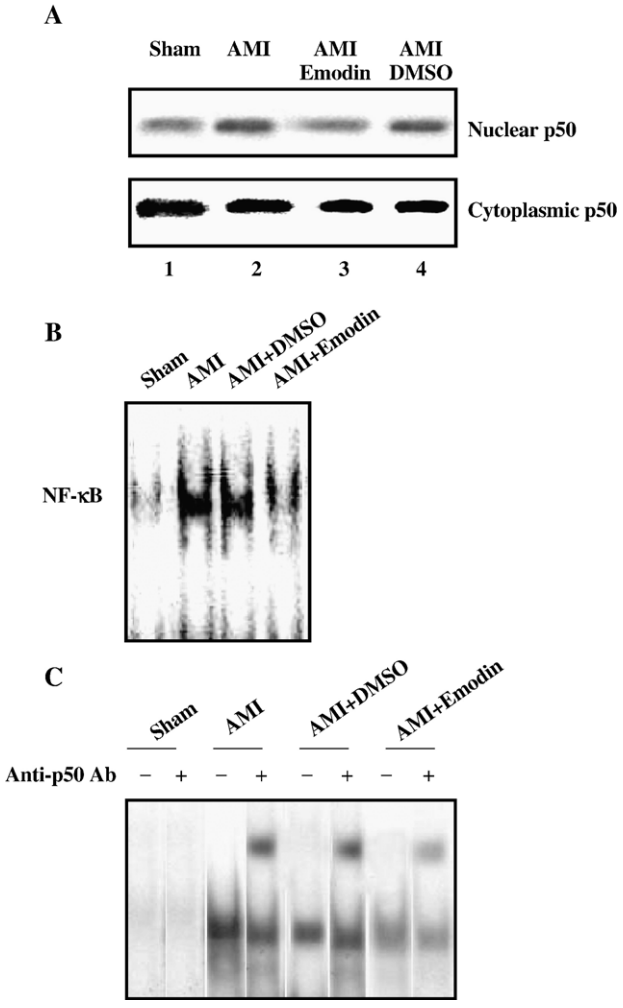


Fig. 3. Effect of emodin on NF-κB binding activity. (A) Changes in p50 expression in nuclear and cytoplasmic extracts ($n=6$) were analyzed by Western blot. All results presented are from independent experiments. (B) Representative EMSA pictures highlighting NF−κB activity of the four groups 2 weeks after MI. (C) Specific NF−κB binding activity and supershift assays were performed using an anti-p50 antibody to investigate the subunit composition of activated NF−κB in infarct myocardium. All results presented are from independent experiments.

Administration of emodin (at concentrations of 15 and 30 mg/kg) reduced MIS/LV to 46.3% ($P<0.05$) and 59.9% ($P<0.05$) of the DMSO-treated MIS, respectively. In addition, administration of emodin at 15 and 30 mg/kg decreased MIS/AAR to 30.7% ($P<0.05$) and 56.2% ($P<0.05$), respectively, of the DMSO-treated MIS (Fig. 1A and B). However, a higher dose of emodin (60 mg/kg) did not result in any further decrease in MIS (data not shown). These results demonstrate that emodin protects mice from AMI.

*Emodin has an anti-inflammatory effect in AMI*

Myocardial infiltration by PMNs and a marker for MPO activity were increased in mice 2 weeks after AMI induction by coronary artery occlusion, but treatment with emodin (30 mg/kg) significantly reduced myocardial PMN infiltration and MPO activity in infarcted myocardium compared with the DMSO-treated group ($P<0.01$) (Fig. 2A, B, and C). Levels of membrane-bound TNF-α protein were significantly decreased in the emodin-treated AMI group (30 mg/kg) at 2 weeks compared with the DMSO-treated AMI group by ELISA analysis ($P<0.05$; Fig. 2D). In addition, emodin (30 mg/kg) also suppressed TNF-α mRNA expression in infarcted myocardial cells by QRT-PCR analysis (Fig. 2E). Immunoblotting of nuclear and cytoplasmic extracts confirmed that emodin (30 mg/kg) decreased nuclear localization of NF-κB p50 2 weeks after AMI (Fig. 3A). NF-κB activity was detected at low levels in the sham group throughout the experiment. In the ischemic myocardium, NF-κB activation was greatly induced 2 weeks after MI. The administration of emodin (30 mg/kg) markedly

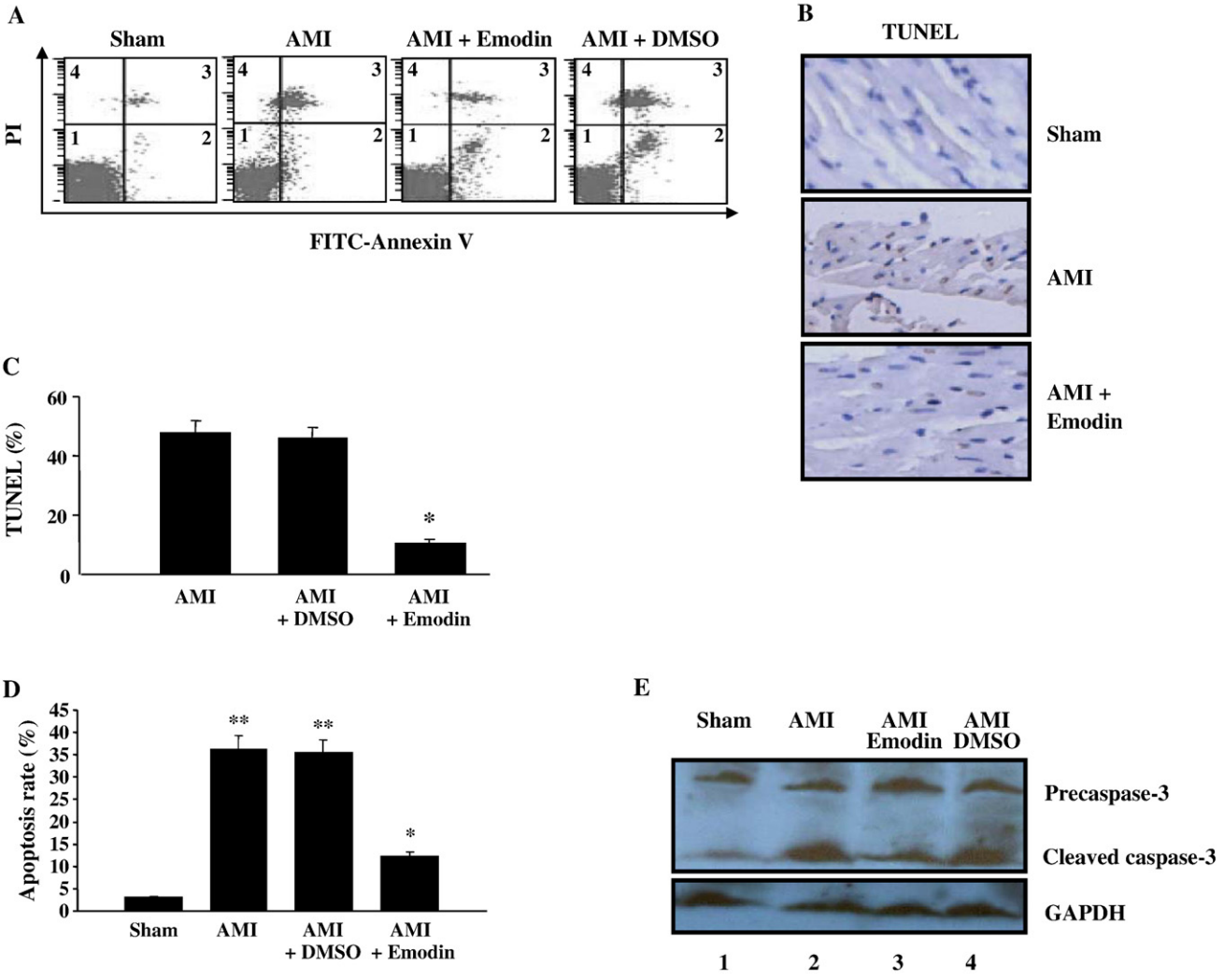


Fig. 4. Emodin protects cells from apoptosis and caspase-3 activation. (A) Myocardial cells ($n=6$) were analyzed by FACS. Viable cardiac cells were negative for both FITC-Annexin V and PI (quadrant 1); early apoptotic cells were labeled by Annexin V, while remaining negative for PI (quadrant 2); late apoptotic cells were positive for both Annexin V and PI (quadrant 3); necrotic cells were labeled by PI, while remaining negative for Annexin V (quadrant 4). The percentage of apoptotic cells includes the early and late apoptotic cells of quadrants 2 and 3. (B) TUNEL-stained myocardial tissue from LV of AMI, emodin-treated AMI, and sham control groups at 2 weeks. (C) Analysis of apoptotic myocardial cells (%) was done using TUNEL staining in the LV at 2 weeks after MI. Data are expressed as a mean±s.e.m. ($n=6$). All results presented are from independent experiments. (D) Quantitative analysis of cardiomyocyte apoptosis in LV by flow cytometric analysis of Annexin V and PI staining. Data are expressed as a mean±s.e.m. ($n=6$). (E) Myocardial caspase-3 activity ($n=6$) was analyzed by Western blot. All results presented are from independent experiments.

attenuated NF-κB activation compared with the DMSO-treated group (Fig. 3B). Incubating the nuclear extracts with an antibody specific to NF-κB (anti-p50 antibody) before addition of the probe resulted in the appearance of slower mobility signals (supershift assay; Fig. 3C). These studies suggest emodin exerts an anti-inflammatory role by suppressing TNF-α expression and NF-κB activation in AMI.

*Emodin has an anti-apoptotic activity in AMI*

Myocardial cell suspension prepared from LV tissue was incubated with Annexin V and PI. Flow cytometric analysis showed reduced apoptosis in myocardial cells treated with emodin (30 mg/kg) than in cells from the AMI group (Fig. 4A). A marked decrease in TUNEL-positive nuclear staining in the sectioned LV myocardium was observed after treatment with emodin (30 mg/kg) compared with the DMSO treatment 2 weeks after AMI. TUNEL-positive nuclear staining was not observed in the sham group (Fig. 4B). The level of apoptosis, as assessed by flow cytometric analysis of TUNEL-positive nuclei in isolated cardiomyocytes, was 12-fold higher 2 weeks after AMI than the sham group (Fig. 4C). The number of apoptotic cells was significantly decreased by treatment with emodin (30 mg/kg) compared with DMSO treatment ($P<0.05$; Fig. 4D). In addition, Western blot analysis indicated that emodin (30 mg/kg) inhibited cleavage of caspase-3 protein 2 weeks after AMI (Fig. 4E). These data indicate that emodin inhibits myocardial cell apoptosis in mice subjected to AMI.

## Discussion

Myocardial infarction causes neutrophil infiltration into the infarct zone and increases the production of proinflammatory cytokines, such as TNF-α (Latini et al., 1994; Nian et al., 2004). Inhibition of neutrophil infiltration could reduce infarct size and attenuate the development of MI (Hoffmeyer et al., 2000). Emodin could be useful in treating various inflammatory diseases (Kumar et al., 1998). Our results indicate that emodin offers protection from myocardial cell injury (Fig. 1) and attenuates PMN infiltration into the infarction area (Fig. 2A, B, and E). Emodin reduced levels of cytoplasmic TNF-α mRNA (Fig. 2C) and membrane-bound TNF-α protein (Fig. 2D). In addition, emodin decreased nuclear localization of nuclear NFκB p50 (Fig. 3A) and markedly suppressed NF-κB activation (Fig. 3B and C). NF-κB is a transcription factor that regulates a battery of inflammatory genes and is a key regulator of the inflammatory response. Activation of NF-κB induces gene programs that lead to transcription of factors that promote inflammation, among them leukocyte adhesion molecules, cytokines such as TNF-α, and chemokines. NF-κB has been reported to be both activated by myocardial IR and involved in IR injury, and both cardiac myocytes and interstitial cells are important sources of NF-κB (Valen, 2004). Proinflammatory cytokines exert their actions on target cells by transactivating NF-κB, so cells such as cardiomyocytes respond to proinflammatory cytokines by activating NF-κB (Baeuerle, 1998). In light of our results, the cardioprotective effect of emodin may be due to reduced neutrophil infiltration and proinflammatory cytokine production via inhibiting NF-κB activity induced by local ischemic injury. Therefore, emodin has a cardioprotective effect related to the inhibition of local myocardial inflammation.

Cardiac apoptosis is a key pathologic feature of AMI. Two major pathways that lead to apoptosis have been identified: the mitochondrial pathway and the death-receptor pathway. Both pathways lead to the activation of caspase-3, a central mediator of the cascade (Abbate et al., 2006). Caspase-3 protein levels are increased in myocardial specimens from patients with right ventricular arrythmogenic dysplasia (Mallat et al., 1996), and caspase-3 is present in its active form in the myocardium of end-stage heart failure patients (Narula et al., 1999). Caspase-3 overexpression predisposes mice to increased myocardial damage after coronary artery ligation when ischemic tissue is reperfused for 24 h, showing a significant increase in infarct size (Condorelli et al., 2001). In mice (Bialik et al., 1997; Sam et al., 2000), cardiac myocyte apoptosis may occur transiently during the first several days after AMI in the ischemic area, whereas LV remodeling later after MI is associated with apoptosis in myocardium remote from the infarct. Recent studies have also shown that amplification of apoptosis was sufficient to increase infarct size, indicating a critical role for cardiomyocyte apoptosis in myocardial infarct expansion (Syed et al., 2005). We demonstrate that myocardial cell apoptosis, measured via TUNEL assay, FITC-Annexin V labeling, and caspase-3 activation, is inhibited by emodin treatment (Fig. 4), implying an anti-apoptotic role for emodin and correlating with protection from myocardial cell injury. Therefore, we speculate that emodin treatment could reduce infarct size due to decreased cardiomyocyte apoptosis in the infarct and peri-infarct region.

Our studies show that PMN infiltration, TNF-α up-regulation, and cardiomyocyte apoptosis in infarcted areas are associated with myocardial infarct size expansion at 2 weeks after MI. Our studies provide evidence that emodin has a novel cardioprotective effect in a murine model of AMI. This protection is conferred, at least partially, by its anti-inflammatory and anti-apoptotic actions in cardiac tissue injury. These studies could provide the basis for a new therapeutic application of emodin to prevent myocardial cell injury in AMI.

## Acknowledgments

We would like to thank Professor Zhang Xiping, from the Department of General Surgery in Hangzhou No. 1 Hospital, for providing the emodin used in this study. This work was supported by grants from the Wuhan Chengguan Science and Technology Project (No. 20055003059-39) in Hubei to Yanxia Wu and Chutian Xuezhe Plan of Hubei in China and Hubei University Foundation in China to Dong-xu Liu.

## References

Abbate, A., Bussani, R., Amin, M.S., Vetrovec, G.W., Baldi, A., 2006. Acute myocardial infarction and heart failure: role of apoptosis. International Journal of Biochemistry & Cell Biology 38, 1834–1840.

Baeuerle, P.A., 1998. IkB–NF-kB structures: at the interface of inflammation control. Cell 95, 729–731.

Baldi, A., Abbate, A., Bussani, R., Patti, G., Melfi, R., Angelini, A., Dobrina, A., Rossiello, R., Silvestri, F., Baldi, F., Di Sciascio, G., 2002. Apoptosis and post-infarction left ventricular remodeling. Journal of Molecular and Cellular Cardiology 34, 165–174.

Bialik, S., Geenen, D.L., Sasson, I.E., Cheng, R., Horner, J.W., Evans, S.M., Lord, E.M., Koch, C.J., Kitsis, R.N., 1997. Myocyte apoptosis during acute myocardial infarction in the mouse localizes to hypoxic regions but occurs independently of p53. Journal of Clinical Investigation 100, 1363–1372.

Chan, T.C., Chang, C.J., Koonchanok, N.M., Geahlen, R.L., 1993. Selective inhibition of the growth of ras-transformed human bronchial epithelial cells by emodin, a protein-tyrosine kinase inhibitor. Biochemical and Biophysical Research Communications 193, 1152–1158.

Chen, R.F., Shen, Y.C., Huang, H.S., Liao, J.F., Ho, L.K., Chou, Y.C., Wang, W.Y., Chen, C.F., 2004. Evaluation of the anti-inflammatory and cytotoxic effects of anthraquinones and anthracenes derivatives in human leucocytes. Journal of Pharmacy and Pharmacology 56, 915–919.

Condorelli, G., Roncarati, R., Ross Jr., J., Pisani, A., Stassi, G., Todaro, M., Trocha, S., Drusco, A., Gu, Y., Russo, M.A., Frati, G., Jones, S.P., Lefer, D.J., Napoli, C., Croce, C.M., 2001. Heart-targeted overexpression of caspase3 in mice increases infarct size and depresses cardiac function. Proceedings of the National Academy of Sciences of the United States of America 98, 9977–9982.

Du, Y., Ko, K.M., 2005. Effects of emodin treatment on mitochondrial ATP generation capacity and antioxidant components as well as susceptibility to ischemia–reperfusion injury in rat hearts: single versus multiple doses and gender difference. Life Sciences 77, 2770–2782.

Frangogiannis, N.G., Smith, C.W., Entman, M.L., 2002. The inflammatory response in myocardial infarction. Cardiovascular Research 53, 31–47.

Hoffmeyer, M.R., Scalia, R., Ross, C.R., Jones, S.P., Lefer, D.J., 2000. PR-39, a potent neutrophil inhibitor, attenuates myocardial ischemia–reperfusion injury in mice. American Journal of Physiology, Heart and Circulatory Physiology 279, H2824–H2828.

Koyama, M., Kelly, T.R., Watanabe, K.A., 1988. Novel type of potential anticancer agents derived from chrysophanol and emodin. Some structure–activity relationship studies. Journal of Medicinal Chemistry 31, 283–284.

Krown, K.A., Page, M.T., Nguyen, C., Zechner, D., Gutierrez, V., Comstock, K.L., Glembotski, C.C., Quintana, P.J., Sabbadini, R.A., 1996. Tumor necrosis factor alpha-induced apoptosis in cardiac myocytes. Involvement of the sphingolipid signaling cascade in cardiac cell death. Journal of Clinical Investigation 98, 2854–2865.

Kumar, A., Dhawan, S., Aggarwal, B.B., 1998. Emodin (3-methyl-1,6,8-trihydroxyanthraquinone) inhibits TNF-induced NF-kappaB activation, IkappaB degradation, and expression of cell surface adhesion proteins in human vascular endothelial cells. Oncogene 17, 913–918.

Latini, R., Bianchi, M., Correale, E., Dinarello, C.A., Fantuzzi, G., Fresco, C., Maggioni, A.P., Mengozzi, M., Romano, S., Shapiro, L., 1994. Cytokines in acute myocardial infarction: selective increase in circulating tumor necrosis factor, its soluble receptor, and interleukin-1 receptor antagonist. Journal of Cardiovascular Pharmacology 23, 1–6.

Li, H.L., Chen, H.L., Li, H., Zhang, K.L., Chen, X.Y., Wang, X.W., Kong, Q.Y., Liu, J., 2005. Regulatory effects of emodin on NF-kappaB activation and inflammatory cytokine expression in RAW 264.7 macrophages. International Journal of Molecular Medicine 16, 41–47.

Lu, J.S., Liu, J.X., Zhang, W.Y., Liang, S.W., Wang, D., Fang, J., 2005. [Preventive effects of emodin on cerebral ischemia injury and expression of the inflammatory factors in rats with cerebral ischemia]. Zhongguo Zhongyao Zazhi 30, 1939–1943.

Mallat, Z., Tedgui, A., Fontaliran, F., Frank, R., Durigon, M., Fontaine, G., 1996. Evidence of apoptosis in arrhythmogenic right ventricular dysplasia. New England Journal of Medicine 335, 1190–1196.

Narula, J., Pandey, P., Arbustini, E., Haider, N., Narula, N., Kolodgie, F.D., Dal Bello, B., Semigran, M.J., Bielsa-Masdeu, A., Dec, G.W., Israels, S., Ballester, M., Virmani, R., Saxena, S., Kharbanda, S., 1999. Apoptosis in heart failure: release of cytochrome *c* from mitochondria and activation of caspase-3 in human cardiomyopathy. Proceedings of the National Academy of Sciences of the United States of America 96, 8144–8149.

Nian, M., Lee, P., Khaper, N., Liu, P., 2004. Inflammatory cytokines and postmyocardial infarction remodeling. Circulation Research 94, 1543–1553.

Palojoki, E., Saraste, A., Eriksson, A., Pulkki, K., Kallajoki, M., Voipio-Pulkki, L.M., Tikkanen, I., 2001. Cardiomyocyte apoptosis and ventricular remodeling after myocardial infarction in rats. American Journal of Physiology. Heart and Circulatory Physiology 280, H2726–H2731.

Sam, F., Sawyer, D.B., Chang, D.L., Eberli, F.R., Ngoy, S., Jain, M., Amin, J., Apstein, C.S., Colucci, W.S., 2000. Progressive left ventricular remodeling and apoptosis late after myocardial infarction in mouse heart. American Journal of Physiology. Heart and Circulatory Physiology 279, H422–H428.

Shiomi, T., Tsutsui, H., Matsusaka, H., Murakami, K., Hayashidani, S., Ikeuchi, M., Wen, J., Kubota, T., Utsumi, H., Takeshita, A., 2004. Overexpression of glutathione peroxidase prevents left ventricular remodeling and failure after myocardial infarction in mice. Circulation 109, 544–549.

Su, H.Y., Cherng, S.H., Chen, C.C., Lee, H., 1995. Emodin inhibits the mutagenicity and DNA adducts induced by 1-nitropyrene. Mutation Research 329, 205–212.

Sun, M., Dawood, F., Wen, W.H., Chen, M., Dixon, I., Kirshenbaum, L.A., Liu, P.P., 2004. Excessive tumor necrosis factor activation after infarction contributes to susceptibility of myocardial rupture and left ventricular dysfunction. Circulation 110, 3221–3228.

Syed, F.M., Hahn, H.S., Odley, A., Guo, Y., Vallejo, J.G., Lynch, R.A., Mann, D.L., Bolli, R., Dorn II, G.W., 2005. Proapoptotic effects of caspase-1/interleukin-converting enzyme dominate in myocardial ischemia. Circulation Research 96, 1103–1109.

Tarnavski, O., McMullen, J.R., Schinke, M., Nie, Q., Kong, S., Izumo, S., 2004. Mouse cardiac surgery: comprehensive techniques for the generation of mouse models of human diseases and their application for genomic studies. Physiological Genomics 16, 349–360.

Torre-Amione, G., 2005. Immune activation in chronic heart failure. American Journal of Cardiology 95, 3C–8C (discussion 38C–40C).

Torre-Amione, G., Stetson, S.J., Youker, K.A., Durand, J.B., Radovancevic, B., Delgado, R.M., Frazier, O.H., Entman, M.L., Noon, G.P., 1999. Decreased expression of tumor necrosis factor-alpha in failing human myocardium after mechanical circulatory support: a potential mechanism for cardiac recovery. Circulation 100, 1189–1193.

Valen, G., 2004. Signal transduction through nuclear factor kappa B in ischemia–reperfusion and heart failure. Basic Research in Cardiology 99, 1–7.

Zhou, X.M., Chen, Q.H., 1988. Biochemical study of Chinese rhubarb. XXII. Inhibitory effect of anthraquinone derivatives on Na+–K+-ATPase of the rabbit renal medulla and their diuretic action. Yaoxue Xuebao 23, 17–20.

Zhou, Y.Y., Wang, S.Q., Zhu, W.Z., Chruscinski, A., Kobilka, B.K., Ziman, B., Wang, S., Lakatta, E.G., Cheng, H., Xiao, P.R., 2000. Culture and adenoviral infection of adult mouse cardiac myocytes: methods for cellular genetic physiology. American Journal of Physiology, Heart and Circulatory Physiology 279, H429–H436.